Progress In Electromagnetics Research, PIER 18, 285–316, 1998

CAVITY MODIFICATIONS OF NUCLEAR INTERNAL CONVERSION RATES

R. W. Ziolkowski

Department of Electrical and Computer Engineering
The University of Arizona
Tucson, AZ 85721-0104, USA

D. M. Gogny

Commissariat a L'Energie Atomique C. E. S. T. A.
Boite postale 2, Le Barp 33114, France

1. INTRODUCTION

Spontaneous emission results from the coupling of an atom to the vacuum modes of the electromagnetic field. However, an atom confined

to a low-loss cavity exhibits radiative properties which differ radically from its free space counterpart. Tuning or detuning the cavity to the atom's transition frequency, one can enhance or inhibit the associated spontaneous emission (SpE) rate of the atom. Cavity quantum electrodynamics studies how these SpE rates can be tailored by the electromagnetic environment into which the atom radiates [1–13]. It has led to a variety of potentially interesting applications including the microcavity laser. Modifications of quantum mechanical behavior in the presence of boundaries have also been studied in conjunction with non-atomic transitions, for instance, with gamma ray emissions from nuclei [14–16] and with the magnetic moment of the electron [17]. We have also recently found that there is experimental evidence [18, 19] of modifications in the decay of the nuclear isomer $235_{92}U$ when it is embedded in silver (a good conductor).

For a cavity tuned near a transition frequency of an atom the SpE rate of that atom is enhanced and is proportional to the Q of the cavity and the wavelength λ_0 of the transition (1): $\Gamma_{cavity} \sim \Gamma_{free}(\lambda_0^3/V)Q$, where Γ_{free} is the SpE rate in vacuum. Similarly, for a cavity de-tuned from a transition frequency the rate is inhibited and is proportional to the inverse of the Q of the cavity (2): $\Gamma_{cavity} \sim \Gamma_{free}(\lambda_0^3/V)Q^{-1}$. As will be shown below with a quantum mechanical derivation, the emissions from an atom or likewise from a nucleus enclosed in a perfect closed cavity can be completely suppressed. They are replaced with Rabi oscillations wherein the emitter-cavity system is in equilibrium; i.e., there is an oscillatory exchange of a photon between the cavity and the atom or nucleus.

In reality, the concept of enhanced and inhibited spontaneous emission is actually restricted to non-closed finite-Q cavities. The SpE rates must be modified if the cavity is in fact open since the available modes include partial bound cavity modes and partial continuum free-space radiation modes. In addition, the coupling of the atom to the free-space modes can occur even in a closed cavity with a finite Q since coupling to the continuum can exist through the lossy walls of the cavity structure. Thus, when the Q of the cavity is not infinite, the modes of the cavity can be coupled to the continuum free-space modes and the Rabi oscillation picture must be modified.

The emission of electromagnetic radiation from an excited nucleus is but one of several channels in which that nucleus can decay from an excited state to a lower energy state. Nuclear transitions having

an energy on the order of 10.0 keV or lower will preferentially decay by means other than photon emission. Internal conversion, like photon emission, is a decay channel for the nucleus which occurs through an electromagnetic process. The vicinity of electrons to the nucleus opens the internal conversion (IC) channel which describes the indirect transfer of the nuclear excitation energy to an electron in one of the various atomic shells and subshells via an intermediate virtual photon transition and its subsequent ejection into an unbound state. Internal conversion is thus a second-order process. It is independent of the photon-emission channels of a nucleus and can be parameterized into an electromagnetic interaction and a nuclear structure part. It becomes a dominant decay channel when atomic electrons are near to the nucleus and the transitions are on the order of 10.0 keV. For instance [20], the IC rate is 1.35×10^4 larger than the photon-emission rate for the 1.642 keV transition of the nuclear isomer $193_{78}Pt$; and it is 3.23×10^4 larger for the 25.98 keV transition of the nuclear isomer $124_{51}Sb$.

Even though it occurs via a virtual photon state, we will show that the rate at which the IC process proceeds can be strongly modified by the presence of a high Q cavity. The IC rates, like the rates for the atomic emissions, depend not only on matching the allowed virtual photon energies to the nuclear transitions, but also on the position of the nucleus. The cavity significantly modifies both of these dependencies. It impacts the size of the matrix coefficients through the position of the nucleus relative to the nodes and anti-nodes of the cavity modes and through the Lorentzian energy distribution of the virtual photons which is peaked or not when the nuclear transition is close or not to the virtual photons allowed by the cavity. The IC rates can be calculated quantum mechanically by analyzing the exchange of the virtual photons that describe the current-current interactions between the electron and nuclear currents. It will be shown that, in principle, the IC rates can be completely suppressed within a perfect cavity if the nucleus is located at nulls of the cavity modes. The more practical influences of lossy cavity walls, hence a finite cavity Q, on the suppression of the IC process are then discussed. These modifications include the broadening of the virtual photon transitions, hence the spacings between the allowed IC channels. Because we are proposing not only modifications of the allowed virtual photon states, but also the transition probability coefficients by the proper positioning of the nuclei, it is concluded that

a practical realization of the cavity IC suppression could be made if a cavity with a sufficiently high Q could be constructed. The Q of the cavity needs to be high only near the nuclear transition frequency under consideration. While still technologically difficult, several potential devices are suggested which would make the realizations of these cavities highly desirable.

It should be noted that the experiments [18, 19] with the nuclear isomer $235_{92}U$ suggest strongly that the local environment does indeed have a major impact on the decay of nuclear transitions. Those experiments indicate that an order of magnitude variation in the lifetime of the $1/2^+$ isomer state of $235_{92}U$ at the $76\,eV$ ($170\,\text{Å}$) transition can be realized. Because the IC rate for this transition in $235_{92}U$ is 200 times larger than the corresponding gamma radiation (photon) process, these experiments indicate that it is possible to modify the IC rates with modifications of the local electromagnetic environment. This further justifies our considerations of the cavity-controlled modifications of the IC rates.

In Section 2 we introduce the ideas concerning the suppression and enhancement of emission from atoms in cavities. While much of this material is known, our presentation allows us to introduce the main concepts and notations, including the situation when the walls of the cavity are lossy. These cavity quantum mechanical concepts are then extended to nuclei in cavities in Section 3. In particular we indicate how the internal conversion process in nuclei can be suppressed by a controlled modification of the electromagnetic environment. This includes both the transverse and longitudinal photon processes associated with internal conversion. Several potential applications for cavity-contrained nuclei that have suppressed or enhanced internal conversion rates are suggested in Section 4. Conclusions are given in Section 5. Many of the detailed calculations have been relegated to a set of appendices so that we may emphasize in these sections the physics of cavity modifications of the internal conversion process rather than the associated mathematics. We would also like to emphasize that the Auger effect, which is a second order decay channel for the atomic transitions, can be similarly modified. The difference is that the Auger transitions occur only through electron current interactions. Nonetheless, all of our analysis applies immediately to this case as well. The cavity suppression of the Auger effect may have its own applications to realizing long-lived pumped states for x-ray laser concepts.

2. ATOM-CAVITY TRANSITION

Consider an atom in a perfectly conducting closed cavity. When the atom radiates, the resulting photon must couple to the intrinsic modes of the cavity to exist. This clearly modifies the emission process when compared to emission into free space since in that case the photon couples to a continuum of radiation modes. To understand the emission process in a closed environment, we must first consider the electromagnetic field in a cavity. Consider an atom in a perfectly conducting closed cubical cavity with side-wall length L. Let the modes of this cavity be labeled by the integers nlm corresponding to the x, y, z directions in the cavity. Since the walls of the cavity are assumed to be perfectly conducting, any electric field within the cavity must vanish on them. Consider the cavity mode functions corresponding (respectively) to the x, y, z directions of the cavity:

$$F^{(1)}_{nlm} = \left(\frac{2}{L}\right)^{3/2} \cos\left(\frac{n\pi}{L}x\right) \sin\left(\frac{l\pi}{L}y\right) \sin\left(\frac{m\pi}{L}z\right) \tag{1a}$$

$$F^{(2)}_{nlm} = \left(\frac{2}{L}\right)^{3/2} \sin\left(\frac{n\pi}{L}x\right) \cos\left(\frac{l\pi}{L}y\right) \sin\left(\frac{m\pi}{L}z\right) \tag{1b}$$

$$F^{(3)}_{nlm} = \left(\frac{2}{L}\right)^{3/2} \sin\left(\frac{n\pi}{L}x\right) \sin\left(\frac{l\pi}{L}y\right) \cos\left(\frac{m\pi}{L}z\right) \tag{1c}$$

To achieve the EM constraints in a cubical cavity, the vector potential takes the form

$$\vec{A}(\vec{x},t) = \sum_{\substack{nlm \\ \epsilon}} \left[\vec{G}^{(\epsilon)}_{nlm}(\vec{x}) A^{(\epsilon)}_{nlm} e^{i\omega_{nlm}t} + \vec{G}^{(\epsilon)*}_{nlm}(\vec{x}) A^{(\epsilon)*}_{nlm} e^{-i\omega_{nlm}t}\right], \tag{2}$$

where the *-sign denotes the complex conjugate and the ω_{nlm} are the natural resonances of the cavity being given by the expression

$$\omega_{nlm} = \frac{\pi}{L} c \left[n^2 + l^2 + m^2\right]^{1/2}, \tag{3}$$

where c is the speed of light in vacuum. The label ϵ represents the polarization state of the EM field. The vector coefficients $\vec{G}^{(\epsilon)}_{nlm}$ are decomposed in terms of the orthogonal coordinate vectors $\vec{e}_1, \vec{e}_2, \vec{e}_3$ as

$$\vec{G}^{(1)}_{nlm}(\vec{x}) = \xi_{11}\vec{e}_1 + \xi_{12}\vec{e}_2 + \xi_{13}\vec{e}_3 \tag{4a}$$

$$\vec{G}^{(2)}_{nlm}(\vec{x}) = \xi_{22}\vec{e}_2 + \xi_{23}\vec{e}_3, \tag{4b}$$

the coefficients ξ_{ij} being linear combinations of the cavity modal functions $F^{(j)}_{nlm}(\vec{x})$:

$$\xi_{11} = -F^{(1)}_{nlm}(\vec{x}) \tag{5a}$$

$$\xi_{12} = +\frac{l}{n} N_{nlm} F^{(2)}_{nlm}(\vec{x}) \tag{5b}$$

$$\xi_{13} = +\frac{m}{n} N_{nlm} F^{(3)}_{nlm}(\vec{x}) \tag{5c}$$

$$\xi_{22} = +\frac{m}{n} N_{nlm} F^{(2)}_{nlm}(\vec{x}) \tag{5d}$$

$$\xi_{23} = -\frac{l}{n} N_{nlm} F^{(3)}_{nlm}(\vec{x}) \tag{5e}$$

where

$$N_{nlm} = \frac{n^2}{l^2 + m^2}. \tag{5f}$$

Consequently, the vector potential satisfies by construction the Coulomb gauge; i.e., by construction $\nabla \cdot \vec{A}(\vec{x}, t) = 0$ because the vector coefficients satisfy the relations

$$\nabla \cdot \vec{G}^{(\epsilon)}_{nlm}(\vec{x}) = 0. \tag{6}$$

We note that with these definitions the vector coefficients are orthogonal:

$$\langle \vec{G}^{(1)}_{nlm}, \vec{G}^{(2)}_{nlm} \rangle = 0 \tag{7a}$$

$$\langle \vec{G}^{(2)}_{nlm}, \vec{G}^{(1)}_{nlm} \rangle = 0 \tag{7b}$$

$$\langle \vec{G}^{(1)}_{nlm} \vec{G}^{(1)}_{nlm} \rangle = 1 + \frac{n^2}{l^2 + m^2} \equiv C^{(1)}_{nlm} \tag{7c}$$

$$\langle \vec{G}^{(2)}_{nlm} \vec{G}^{(2)}_{nlm} \rangle = \frac{n^2}{l^2 + m^2} \equiv C^{(2)}_{nlm} \tag{7d}$$

where $\langle \bullet, \bullet \rangle$ represents the inner product over the cavity.

The magnetic flux and electric fields follow immediately from the vector potential:

$$\vec{B} = \nabla \times \vec{A} \tag{8a}$$

$$\vec{E} = -\partial_t \vec{A}. \tag{8b}$$

With these expressions we calculate in the usual manner the energy of the electromagnetic field:

$$H_{EM} = \frac{\epsilon_0}{2} \int_V \left[|\vec{E}(\vec{x},t)|^2 + c^2 |\vec{B}(\vec{x},t)|^2 \right] d^3\vec{x}. \tag{9}$$

With $\vec{A}$ given by Eq. (2) and the orthogonality conditions (7), the energy (9) follows from the field quantities (8) as

$$U_{EM} = \epsilon_0 \sum_{\substack{nlm \\ \epsilon}} \omega_{nlm}^2 C_{nlm}^{(\epsilon)} \left(A_{nlm}^{(\epsilon)} A_{nlm}^{(\epsilon)*} + A_{nlm}^{(\epsilon)*} A_{nlm}^{(\epsilon)} \right). \tag{10}$$

To express this result in a quantum mechanical oscillator form, we introduce the normalized quantities:

$$a_{nlm}^{(\epsilon)} = \left[\frac{\hbar}{2\epsilon_0 \omega_{nlm} C_{nlm}^{(\epsilon)}} \right]^{-1/2} A_{nlm}^{(\epsilon)} \tag{11a}$$

$$a_{nlm}^{(\epsilon)*} = \left[\frac{\hbar}{2\epsilon_0 \omega_{nlm} C_{nlm}^{(\epsilon)}} \right]^{-1/2} A_{nlm}^{(\epsilon)*} \tag{11b}$$

This allows us to rewrite the energy (10) as

$$U_{EM} = \sum_{\substack{nlm \\ \epsilon}} \frac{\hbar\omega_{nlm}}{2} \left(a_{nlm}^{(\epsilon)} a_{nlm}^{(\epsilon)*} + a_{nlm}^{(\epsilon)*} a_{nlm}^{(\epsilon)} \right). \tag{12}$$

To express this result in quantum mechanical (second quantized) form, we identify the constants $a_{nlm}^{(\epsilon)}$ and $a_{nlm}^{(\epsilon)*}$ with, respectively, the annihilation and creation operators $\hat{a}_{nlm}^{(\epsilon)}$ and $\hat{a}_{nlm}^{(\epsilon)\dagger}$ for a photon with polarization ϵ in the nlm-cavity mode so that the energy (12) then gives us the quantum mechanical Hamiltonian for the photons:

$$H_\gamma = \sum_{\substack{nlm \\ \epsilon}} \frac{\hbar\omega_{nlm}}{2} \left(\hat{a}_{nlm}^{(\epsilon)} \hat{a}_{nlm}^{(\epsilon)\dagger} + \hat{a}_{nlm}^{(\epsilon)\dagger} \hat{a}_{nlm}^{(\epsilon)} \right). \tag{13}$$

In addition, we obtain the quantum mechanical vector potential:

$$\vec{A}(\vec{x},t) = \sum_{\substack{nlm \\ \epsilon}} \vec{\Lambda}_{nlm}^{(\epsilon)}(\vec{x}) e^{i\omega_{nlm}t} \hat{a}_{nlm} + \vec{\Lambda}_{nlm}^{(\epsilon)*}(\vec{x}) e^{-i\omega_{nlm}t} \hat{a}_{nlm}^\dagger \tag{14}$$

where the vector coefficients are now

$$\vec{\Lambda}^{(\epsilon)}_{nlm}(\vec{x}) = \left(\frac{\hbar}{2\epsilon_0 C^{(\epsilon)}_{nlm}\omega_{nlm}}\right)^{1/2} \vec{G}^{\epsilon}_{nlm}(\vec{x}) \tag{15}$$

As shown in Appendix A, with these expressions one can calculate the energy in the cavity and the Q of a lossy cavity. The volume stored energy

$$\mu_0 \sum_{\epsilon} \iiint |\vec{H}^{\epsilon}_{nlm}|^2 d^3\vec{x} = \hbar\omega_{nlm} \tag{16}$$

gives the expected energy in the photon mode. Moreover, if the walls of the cavity are not perfect, the cavity modes couple to the wall and to the continuum through the walls. Thus, we expect that there will be a broadening of the cavity resonances:

$$\omega_{nlm} = \omega^R_{nlm} - i\Gamma_{nlm} \tag{17}$$

where ω^R_{nlm} is the real part of the mode frequency and the line width (Half Width at Half Max) of this transition frequency is obtained perturbatively as

$$\Gamma_{nlm} = \frac{\sum_{\epsilon} \iint \mathrm{Re}(Z_{wall})|\vec{H}^{\epsilon}_{nlm}|^2\, dS}{\mu_0 \sum_{\epsilon} \iiint |\vec{H}^{\epsilon}_{nlm}|^2\, d^3\vec{x}}. \tag{18}$$

The Q associated with a particular nlm-cavity mode follows from this natural line width as $Q = \omega^R_{nlm}/\Gamma_{nlm}$.

Assuming that the electric and magnetic fields are related through the wall impedance, i.e., $E_{wall} = Z_{wall}H_{wall}$, the line width becomes

$$\Gamma_{nlm} = \frac{8\mathrm{Re}(Z_{wall})}{\mu_0 L} = \frac{8\mathrm{Re}(Z_{wall})}{\sqrt{\epsilon_0\mu_0}L}\sqrt{\frac{\epsilon_0}{\mu_0}} = 8\left(\frac{c}{L}\right)\frac{\mathrm{Re}(Z_{wall})}{Z_0} \tag{19}$$

where $Z_0 = (\mu_0/\epsilon_0)^{1/2}$ is the characteristics wave impedance of free space. If the walls are made from metals with very high conductivity, the wall impedance has a real part

$$\mathrm{Re}(Z_{wall}) = \sqrt{\frac{\omega^R_{nlm}\mu_0}{2\sigma}} \tag{20}$$

so that Q can be written as

$$Q = \frac{\omega_{nlm}}{\Gamma_{nlm}} = \frac{L}{\sqrt{3\tilde{2}}c}\sqrt{\frac{\sigma}{\epsilon_0}}\sqrt{\omega_{nlm}^R} \tag{21}$$

As shown in Appendix B, this quantum mechanical value agrees with the classical result.

Now if we want to understand a little how the presence of the cavity modifies the transition probabilities of the spontaneous emission, we write the Hamiltonian in the form:

$$H = H_{atom} + H_\gamma + H_{int} \tag{22}$$

where H_{atom} is the unperturbed Hamiltonian of the atom and H_γ is given by (13). The interaction Hamiltonian operator H_{int} is, of course, the second quantized form of the interaction term

$$H_{int} = -\int d^3\vec{x}\, \vec{J}_{atom}(\vec{x}) \cdot \vec{A}_\gamma(\vec{x}) \tag{22'}$$

The vector potential of the photon $\vec{A}_\gamma$ is given by (14); $\vec{J}_{atom}$ is the current associated with the electron transitions in the atom. For the sake of simplicity we will restrict the discussions below to electronic transitions and deal only with electric dipole interactions. In the interaction picture we readily obtain the rate of transitions from an initial atomic state i with zero photons (labeled $|i,0\rangle$) to a final atomic state f with a single photon propagating into the $\vec{k}$ direction with polarization ϵ (labeled $|f,1_{\vec{k},\epsilon}\rangle$). In the free space case the result is simply the (Fermi) Golden Rule:

$$\Gamma_{i\to f}^{free} = \frac{2\pi}{\hbar}\sum_\epsilon \int d^3\vec{k} \left|\langle f,1_{\vec{k},\epsilon}|\hat{H}_{int}|i,0\rangle\right|^2 \delta(E_{\vec{k}} - E_{fi}), \tag{23}$$

where the photon energy $E_{\vec{k}} = \hbar\omega$ and the transition energy $E_{fi} = E_f - E_i$. Note that we have summed over all possible polarization states of the emitted photons. Let

$$\vec{G}_{\vec{k}}^{(\epsilon)}(\vec{x}) = \left(\frac{1}{2\pi}\right)^{3/2} e^{i\vec{k}\cdot\vec{x}}\, \vec{c}_{\vec{k}} \tag{24}$$

be the plane wave vector expansion coefficient for a wave propagating into the $\vec{k}$ direction, $\vec{\epsilon}_{\vec{k}}$ being the associated polarization vector. The transition matrix in (23) has the form

$$\sum_{\epsilon} \left| \langle f, 1_{\vec{k},\epsilon} | \hat{H}_{int} | i, 0 \rangle \right|^2 = \frac{e^2}{m^2} \frac{\hbar}{2\epsilon_0 \omega_{\vec{k}}} \sum_{\epsilon} \left[C_{\vec{k}}^{(\epsilon)} \right]^{-1} \times \left| \int d^3\vec{x} \langle f | \vec{p}(\vec{x}) | i \rangle \cdot \vec{G}_{\vec{k}}^{(\epsilon)}(\vec{x}) \right|^2, \quad (25)$$

where $\vec{p}$ is the momentum of the transition electron and $\hbar\vec{k}$ represents the momentum of the free-space photon. The normalization constant $C_{\vec{k}}^{(\epsilon)} = 1$ for this plane wave case. Let us assume that we have an ensemble of atoms whose orientations are randomly distributed. If we take the dipole approximation, i.e., we take the electromagnetic field variation to be small across the position of the n-th atom $\vec{x}_n$, and if we integrate over these random orientations, we obtain

$$\left| \int d^3\vec{x} \langle f | \vec{p}(\vec{x}) | i \rangle \cdot \vec{G}_{\vec{k}}^{(\epsilon)}(\vec{x}) \right|^2 = \frac{1}{3} |\vec{G}_{\vec{k}}^{(\epsilon)}(\vec{x}_A)|^2 \left| \int d^3\vec{x} \langle f | \vec{p}(\vec{x}) | i \rangle \right|^2 = \frac{(m\omega_{\vec{k}})^2}{3} |\vec{G}_{\vec{k}}^{(\epsilon)}(\vec{x}_A)|^2 \, |\vec{d}_{fi}|^2, \quad (26)$$

where $\vec{d}_{fi}$ is the dipole matrix element of the transition between the initial and final states. Introducing the Einstein coefficient for spontaneous emission

$$A_{i\to f}(\omega) = \frac{e^2 \omega^3 |\vec{d}_{fi}|^2}{3\pi\epsilon_0 \hbar c^3}, \quad (27)$$

the transition rate at the location of the atom becomes simply

$$\Gamma_{i\to f}^{free}(\vec{x}_A) = \frac{\hbar\pi c^3}{\omega_{\vec{k}}^2} A_{i\to f}(\omega_{\vec{k}}) \sum_{\epsilon} \int dk \, k^2 \frac{|\vec{G}_{\vec{k}}^{(\epsilon)}(\vec{x}_A)|^2}{C_{\vec{k}}^{(\epsilon)}} \delta(E_{\vec{k}} - E_{fi}). \quad (28)$$

In contrast, the cavity supports only a discrete set of modes, thus limiting the emission possibilities. The corresponding transition rate from the initial atomic state with zero photons, $|i, 0\rangle$, to the final atomic state with a single photon in the nlm-mode of the cavity with polarization ϵ, $|f, 1_{nlm,\epsilon}\rangle$, is simply

$$\Gamma_{i\to f}^{cavity} = \frac{2\pi}{\hbar} \sum_{\substack{nlm \\ \epsilon}} \left| \langle f, 1_{nlm,\epsilon} | \hat{H}_{int} | i, 0 \rangle \right|^2 \delta(E_{nlm} - E_{fi}), \quad (29a)$$

which gives in the dipole approximation the rate of emission

$$\Gamma_{i\to f}^{cavity}(\vec{x}_A) = \frac{\hbar\pi c^3}{\omega_{nlm}^2} A_{i\to f}(\omega_{nlm}) \sum_{\substack{nlm \\ \epsilon}} \frac{|\vec{G}_{nlm}^{(\epsilon)}(\vec{x}_A)|^2}{C_{nlm}^{(\epsilon)}} \delta(E_{nlm} - E_{fi}). \quad (29b)$$

Clearly the difference in the transition rates into free space (27) and into a cavity mode (29) lies in the difference in nature of the cavity vector coefficients, i.e., the differences between, respectively, $\vec{G}_{\vec{k}}^{(\epsilon)}(\vec{x}_A)$ and $\vec{G}_{nlm}^{(\epsilon)}(\vec{x}_A)$, and the allowed transition energies $E_{\vec{k}} = \hbar\omega_{\vec{k}}$ and $E_{nlm} = \hbar\omega_{nlm}$. It has been shown that these differences can lead to inhibition or enhancement of the transition rates [3–13].

Now if the cavity is lossy, the Hamiltonian (22) must be modified to the form

$$H = H_{atom} + H_\gamma + H_{int}^{atom} + H_{int}^{wall} \quad (30)$$

where H_{int}^{atom} is given by Eq. (22′) and

$$H_{int}^{wall} = -\int d^3\vec{x}\, \vec{J}_{wall}(\vec{x}) \cdot \vec{A}_\gamma(\vec{x}) \quad (30')$$

$\vec{J}_{wall}$ being the currents associated with the electron transitions in the walls. If we treat the atom-cavity system semi-classically, we find that the effect of the wall interaction term H_{int}^{wall} is to shift and broaden the photon spectrum. We find that

$$H = H_{atom} + \frac{1}{2}\sum_{\substack{nlm \\ \epsilon}} \hbar(\omega_{nlm}^R - i\Gamma_{nlm}) \left(\hat{a}_{nlm}^{(\epsilon)}\hat{a}_{nlm}^{(\epsilon)\dagger} + \hat{a}_{nlm}^{(\epsilon)\dagger}\hat{a}_{nlm}^{(\epsilon)}\right) + H_{int}^{atom} \quad (31)$$

where ω_{nlm}^R and Γ_{nlm} are defined, respectively, by Eqs. (17) and (18). This means that if we were to calculate the transition probability, the difference between the conservation of energy in an infinitely narrow line and the atom-cavity transition is the presence of the broadening term

$$\frac{\Gamma_{nlm}}{(E_{fi} - \hbar\omega_{nlm}^R)^2 + \Gamma_{nlm}^2} \quad (32)$$

rather than simply the on-shell result $\delta(E_{fi} - \hbar\omega_{nlm})$ corresponding to the one present in Eqs. (28) and (29). This is confirmed with a quantum calculation in Appendix A and a classical circuits approach in Appendix B.

3. INTERNAL CONVERSION OF AND SPONTANEOUS EMISSION FROM A NUCLEUS IN A CAVITY

In the case of a nucleus, the decay of an excited state can proceed not only via spontaneous emission of a real photon, but also via a virtual photon transition. This process is called internal conversion. In order to study the stability of an excited state of a nucleus in a cavity, we must determine the cavity modifications of the internal conversion process rates.

3.1 Internal Conversion for a Nucleus in Free Space

Internal conversion (IC) in an excited nucleus is a second order process by which an electron which orbits the nucleus is ejected into the continuum when the nucleus decays to a lower energy state. It occurs via a virtual photon interaction between the nucleus and the electron. To understand the basic physics of the IC process when the excited nucleus is contained in a closed cavity, we proceed as we did above with the atom-cavity system and consider first the Hamiltonian for a nucleus-electron system in free space:

$$H = H_N + H_e + H_\gamma + H_{int} \tag{33}$$

where H_N is the unperturbed Hamiltonian of the nucleus; H_e is the unperturbed Hamiltonian of the electron involved in the internal conversion process; H_γ is again the Hamiltonian for the photon; and H_{int} is the interaction Hamiltonian which now has the form:

$$H_{int} = -\int \left[\vec{j}_e^{\perp}(\vec{x}) \cdot \vec{A}_N^{\perp}(\vec{x}) + \vec{j}_N^{\perp}(\vec{x}) \cdot \vec{A}_e^{\perp}(\vec{x})\right] d^3\vec{x}. \tag{34}$$

We have chosen to omit for the moment the Coulomb force terms in the interaction Hamiltonian between the nucleus and the electron which play an essential role for the K-shell electrons and when the IC process is very weak or non-existent. We will come back to those terms below.

The terms in the interaction Hamiltonian (34) represent respectively the perpendicular components of the electron current $\vec{j}_e^{\perp}(\vec{x})$, the nuclear current $\vec{j}_N^{\perp}(\vec{x})$, the vector potential arising from the electron current $\vec{A}_e^{\perp}(\vec{x})$, and the vector potential arising from the nuclear current $\vec{A}_N^{\perp}(\vec{x})$. In the interaction picture the wave function for this system can be expressed in terms of the interaction Hamiltonian as

$$\Psi_I(t) = \Psi_I(t_0) - \frac{i}{\hbar}\int_{t_0}^{t} H_{int}(t')\Psi_I(t')dt'. \tag{35}$$

The associated perturbation sequence to second order is

$$\begin{aligned}\Psi_I(t) \approx & \Psi_I(t_0) - \frac{i}{\hbar}\int_{t_0}^{t} H_{int}(t')dt'\Psi_I(t_0) \\ & -\frac{1}{\hbar^2}\int_{t_0}^{t} dt' \int_{t_0}^{t} dt''\Theta(t'-t'')H_{int}(t')H_{int}(t'')\Psi_I(t_0) + \ldots\end{aligned} \tag{36}$$

where $\Theta(t'-t'')$ is the Heaviside function and guarantees the proper time ordering. We set $\Psi_I(t_0) \equiv \Psi_i = |\phi_i\psi_\alpha 0\rangle$ to be the initial state consisting of the electron in the bound state ϕ_i, the nucleus in the excited state ψ_α, and zero photons. We also set $\Psi_I(t) \equiv \Psi_f = \langle 0\ \psi_\beta\phi_f|$ to be the final state consisting of the electron in an unbound, continuum state ϕ_f, the nucleus in the de-excited state ψ_β, and again zero photons. The photons in the intermediate state occur in the free-space case in a completely open region and are labeled by the continuum plane wave wavenumber direction $\vec{k}$ and polarization state ϵ. To determine the rate of the IC process, we need to generate the matrix element

$$\langle\Psi_f|\hat{H}_{int}|\Psi_i\rangle = \langle\Psi_f|\hat{H}^{(1)}_{int}|\Psi_i\rangle + \langle\Psi_f|\hat{H}^{(2)}_{int}|\Psi_i\rangle, \tag{37}$$

where $\hat{H}^{(1)}_{int}$ and $\hat{H}^{(2)}_{int}$ represent the first and second order interaction operator terms in the perturbation sequence (36).

With several standard manipulations which mimic the procedures given in Ref. 21, we obtain the first order expression

$$\begin{aligned}\langle\Psi_f|\hat{H}^{(1)}_{int}|\Psi_i\rangle &= -\frac{i}{\hbar}\int_{t_0}^{t} dt'\langle 0\psi_\beta\phi_f|H_{int}(t')|\phi_i\psi_\alpha 0\rangle \\ &= -2\pi i\langle 0\psi_\beta\phi_f|\hat{H}_{int}|\phi_i\psi_\alpha 0\rangle\delta^{(T)}(E_{fi}-E_{\alpha\beta}),\end{aligned} \tag{38}$$

where $E_{fi} = E_f - E_i$ and $E_{\alpha\beta} = E_\alpha - E_\beta$ and where we have chosen the times symmetrically as $t = T/2$ and $t_0 = -T/2$ so that we can write the approximate delta function $\delta^{(T)}(E)$ in (38) as

$$\delta^{(T)}(E) = \frac{\sin(ET/2\hbar)}{\pi E} \tag{39}$$

Because the final and initial states contain no photons and the vector potentials contained in the operator H_{int} contain single creation or annihilation operators, the first order interaction matrix element (38) is identically zero:

$$\langle\Psi_f|\hat{H}^{(1)}_{int}|\Psi_i\rangle \equiv 0. \tag{40}$$

The second order term follows in a similar but more tedious manner:

$$\begin{aligned}
&\langle\Psi_f|\hat{H}_{int}^{(2)}|\Psi_i\rangle \\
&\quad = -\frac{1}{\hbar^2}\int_{t_0}^{t} dt' \int_{t_0}^{t} dt''\Theta(t'-t'')\langle 0\psi_\beta\phi_f|H_{int}(t')H_{int}(t'')|\phi_i\psi_\alpha 0\rangle \\
&\quad = -\frac{1}{\hbar^2}\int_{t_0}^{t} dt' \int_{t_0}^{t} dt''\Theta(t'-t'')e^{i(E_\beta+E_f)t'/\hbar}\ e^{-i(E_\alpha+E_i)t''/\hbar} \\
&\qquad \times \langle 0\psi_\beta\phi_f| \int d^3\vec{x}\left[\vec{j}_e^{\perp}(\vec{x})\cdot\vec{A}_N^{\perp}(\vec{x}) + \vec{j}_N^{\perp}(\vec{x})\cdot\vec{A}_e^{\perp}(\vec{x})\right] \\
&\qquad \times e^{-i(H_0+H_\gamma)t'/\hbar}\ e^{i(H_0+H_\gamma)t''/\hbar} \\
&\qquad \times \int d^3\vec{x}'\left[\vec{j}_e^{\perp}(\vec{x}')\cdot\vec{A}_N^{\perp}(\vec{x}') + \vec{j}_N^{\perp}(\vec{x}')\cdot\vec{A}_e^{\perp}(\vec{x}')\right]|\phi_i\psi_\alpha 0\rangle, \qquad (41)
\end{aligned}$$

In a manner similar to the treatment of the emission of a photon by an atom we decompose, for example, the vector potential associated with the electron currents into the allowed continuum radiation modes

$$\vec{A}_e^{\perp}(\vec{x}) = \int d^3\vec{k}\left(\frac{\hbar}{2\epsilon_0\omega_{\vec{k}}}\right)^{1/2}\left[\vec{G}_{\vec{k}}^{(\epsilon)}(\vec{x})\hat{a}_{\vec{k}} + \vec{G}_{\vec{k}}^{(\epsilon)\ *}(\vec{x})\vec{a}_{\vec{k}}^{\dagger}\right], \qquad (42)$$

where we again have the vector coefficients $\vec{G}_{\vec{k}}^{(\epsilon)}(\vec{x})$ given by Eq. (24). The second order interaction matrix element (41) then becomes

$$\begin{aligned}
\langle\Psi_f|\hat{H}_{int}^{(2)}|\Psi_i\rangle = &-\frac{1}{\hbar^2}\sum_{\epsilon}\int d^3\vec{k}\ X_{\beta\alpha}^{*}(\vec{k},\ \epsilon)X_{fi}(\vec{k},\ \epsilon)\Lambda_{\beta\alpha,\ fi}^{(1)}(t,\ t_0) \\
&-\frac{1}{\hbar^2}\sum_{\epsilon}\int d^3\vec{k}\ X_{\beta\alpha}(\vec{k},\ \epsilon)X_{fi}^{*}(\vec{k},\ \epsilon)\Lambda_{\beta\alpha,\ fi}^{(2)}(t,\ t_0),
\end{aligned} \qquad (43)$$

where the individual nuclear and electronic matrix elements are

$$X_{\beta\alpha}(\vec{k},\ \epsilon) = \left(\frac{\hbar}{2\epsilon_0\omega_{\vec{k}}}\right)^{1/2}\int d^3\vec{x}'\langle\psi_\beta|\vec{j}_N^{\perp}(\vec{x}')\cdot\vec{G}_{\vec{k}}^{(\epsilon)}(\vec{x}')|\psi_\alpha\rangle \qquad (44a)$$

$$X_{fi}(\vec{k},\ \epsilon) = \left(\frac{\hbar}{2\epsilon_0\omega_{\vec{k}}}\right)^{1/2}\int d^3\vec{x}'\langle\phi_f|\vec{j}_e^{\perp}(\vec{x}')\cdot\vec{G}_{\vec{k}}^{(\epsilon)}(\vec{x}')|\phi_i\rangle \qquad (44b)$$

where E_γ is the energy of the virtual photon which carries the interaction between the nucleus and the electron. The time functions explicitly yield the conservation of energy:

$$\Lambda^{(1)}_{\beta\alpha,\ fi}(t,\ t_0) = \int_{t_0}^{t} dt' e^{i(E_{fi}-E_\gamma)t'/\hbar} \int_{t_0}^{t} dt'' \Theta(t'-t'') e^{i(E_\gamma - E_{\alpha\beta})t''/\hbar}$$
$$= 2\pi\hbar^2 \lim_{\eta\to 0_+} \frac{\delta^{(T)}(E_{fi}-E_{\alpha\beta})}{E_{\alpha\beta}-E_\gamma+i\eta} \tag{45a}$$

$$\Lambda^{(2)}_{\beta\alpha,\ fi}(t,\ t_0) = \int_{t_0}^{t} dt' e^{-i(E_\gamma - E_{\alpha\beta})t'/\hbar} \int_{t_0}^{t} dt'' \Theta(t'-t'') e^{-i(E_{fi}-E_\gamma)t''/\hbar}$$
$$= 2\pi\hbar^2 \lim_{\eta\to 0_+} \frac{\delta^{(T)}(E_{fi}+E_{\alpha\beta})}{-(E_{\alpha\beta}+E_\gamma)+i\eta}. \tag{45b}$$

where again we have explicitly taken $t = T/2$ and $t_0 = -T/2$. Therefore we obtain

$$\langle \Psi_f | \hat{H}^{(2)}_{int} \Psi_i \rangle =$$
$$-\frac{2\pi i}{\hbar} \lim_{\eta\to 0_+} \left\{ \begin{array}{l} \displaystyle\sum_\epsilon \int d^3\vec{k} \frac{X^*_{\beta\alpha}(\vec{k},\ \epsilon) X_{fi}(\vec{k},\ \epsilon)}{E_{\alpha\beta}-E_\gamma+i\eta} \delta^{(T)}(E_{fi}-E_{\alpha\beta}) \\ \displaystyle + \sum_\epsilon \int d^3\vec{k} \frac{X_{\beta\alpha}(\vec{k},\ \epsilon) X^*_{fi}(\vec{k},\ \epsilon)}{-(E_{\alpha\beta}+E_\gamma)+i\eta} \delta^{(T)}(E_{fi}-E_{\alpha\beta}) \end{array} \right\}. \tag{46}$$

This result agrees, modulo the Coulomb force terms, with Eq. (10.35) of Ref. 22. The Feynman diagrams for the two terms in this matrix element are shown in Figure 1.

3.2 Internal Conversion for a Nucleus in a Cavity

Reconsidering the IC process in our cubical cavity, the modes available to the virtual photon are now restricted by the presence of the perfectly conducting walls. In particular, the possible energy of the virtual photon is now restricted to the natural resonant frequencies of the cavity E_{nlm}. The first order perturbation result is again identically zero. The corresponding cavity second order interaction matrix element is straightforwardly obtained in the same manner as (46):

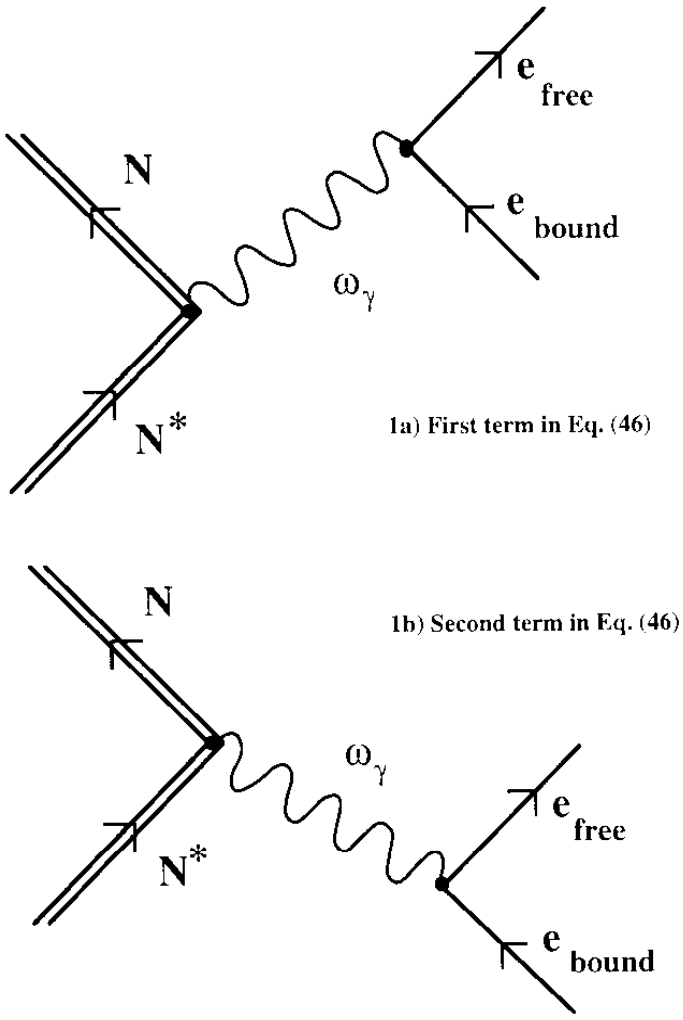

Figure 1. Feynman diagrams corresponding to the internal conversion process.

$$\langle \Psi_f | \hat{H}_{int}^{(2)} \Psi_i \rangle =$$
$$-\frac{2\pi i}{\hbar} \lim_{\eta \to 0_+} \left\{ \sum_{\substack{nlm \\ \epsilon}} \left[\frac{X^*_{\beta\alpha}(nlm;\ \epsilon) X_{fi}(nlm;\ \epsilon)}{E_{\alpha\beta} - E_{nlm} + i\eta} \delta^{(T)}(E_{fi} - E_{\alpha\beta}) \right. \right.$$
$$\left. \left. + \frac{X_{\beta\alpha}(nlm;\ \epsilon) X^*_{fi}(nlm;\ \epsilon)}{-(E_{\alpha\beta} + E_{nlm}) + i\eta} \delta^{(T)}(E_{fi} - E_{\alpha\beta}) \right] \right\}. \tag{47}$$

where the individual nuclear and electronic matrix elements are now

$$X_{\beta\alpha}(nlm;\ \epsilon) = \left(\frac{\hbar}{2\epsilon_0\omega_{nlm}}\right)^{1/2} \int d^3\vec{x}' \langle\psi_\beta|\vec{j}_N^{\perp}(\vec{x}') \cdot \vec{G}^{(\epsilon)}_{nlm}(\vec{x}')|\psi_\alpha\rangle \tag{48a}$$

$$X_{fi}(nlm;\ \epsilon) = \left(\frac{\hbar}{2\epsilon_0\omega_{nlm}}\right)^{1/2} \int d^3\vec{x}' \langle\phi_f|\vec{j}_e^{\perp}(\vec{x}) \cdot \vec{G}^{(\epsilon)}_{nlm}(\vec{x})|\phi_i\rangle. \tag{48b}$$

Clearly the differences in the transition matrices between the free space and the cavity environments again appear, respectively, through the field coefficients, $\vec{G}^{(\epsilon)}_{\vec{k}}(\vec{x})$ and $\vec{G}^{(\epsilon)}_{nlm}(\vec{x})$, and the transition frequencies $\omega_{\vec{k}}$ and ω_{nlm}. These differences will be lead to different IC rates.

Calculating the current matrix elements (48a) or (48b), we find that the IC process can be completely suppressed when the nucleus is confined to a closed, perfect cavity and placed in particular locations. As shown in Appendix D, if we introduce the nucleon transition current

$$\vec{J}_{\beta\alpha} = -i\hbar\left(\frac{q}{M}\right)_N \sum_i \int d^3\vec{x}' d^3\vec{x}_1 \ldots d^3\vec{x}_i \ldots d^3\vec{x}_n \left[\psi^*_\beta(\vec{x}_1, \ldots, \vec{x}_i, \ldots, \vec{x}_n) \times\delta(\vec{x}' - \vec{x}_i)\nabla_{\vec{x}_i}\psi_\alpha(\vec{x}_1, \ldots, \vec{x}_i, \ldots, \vec{x}_n)\right], \tag{49}$$

and recognize that because the nucleus is highly localized in the cavity so that it experiences only minute variations in the field, then the nuclear current matrix element becomes

$$X_{\beta\alpha}(nlm;\ \epsilon) \approx \left(\frac{\hbar}{2\epsilon_0\omega_{nlm}}\right)^{1/2} \vec{G}^{(\epsilon)}_{nlm}(\vec{x}_N) \cdot \vec{J}_{\beta\alpha}. \tag{50}$$

Therefore, for example, when the nucleus is located at $\vec{x}_N = (L/2,\ L/2,\ L/2)$, the IC matrix element is zero and, hence, the IC process is completely suppressed. Simply by locating the nuclei at a null or at a peak of the cavity modal coefficients, one can inhibit or enhance the IC electron emission rate. We note that for the perfect cavity the IC suppression is also true for the extremely high mode numbers. For these high mode numbers, we would return to (48a) and recognize that the field coefficients will be highly oscillatory over the position of the nucleons and, hence, would give zero in general. Moreover, it is apparent from Eq. (47) that it is not important to include these

high mode numbers in the sum since they contribute little to the final result. In fact we find that if the nuclear transition frequency is not close enough to a cavity mode frequency, then the coupling to the cavity modes will be weak and the IC matrix element will again be very small. It is important to note that if the walls are lossy but the Q of the cavity remains large for the nuclear transition frequency of interest, this result will change little because the cavity's modal functions will remain essentially the same. The transitions acquire widths corresponding to a particular density of states, but will remain highly localized.

Thus we find that the value of the IC matrix elements for a nucleus in a cavity will be highly position dependent. By simply locating the nuclei at a null or at a peak of the cavity modal coefficients, one can inhibit or enhance the IC electron emission rate. These results obviously imply that the presence of the cavity walls can significantly alter the IC process. We emphasize that this occurs even though the exchange process involves a virtual photon emission and reabsorption.

When the cavity is open, the matrix elements of the IC process will attain values somewhere between Eqs. (46) and (47). Suppression or enhancement of the IC rates will be possible as one approaches the cavity case. If the cavity is only slightly open, the modal functions experience little modification and the matrix elements will attain values very close to those in (50). The normal IC process occurs within the near field of the radiation modes associated with free space, i.e., near the nucleus. In the cavity IC process the radiation modes are restricted to the "near field" since the modes are confined to the cavity region, even if it is slightly open. Nonetheless, these modes are connected to the region exterior to the cavity via its aperture. Real photons are now realizable in the exterior region, particularly at the resonance modes of the cavity where resonant coupling to the exterior is possible [23–24]. If the nucleus was placed at a peak of a cavity mode and the transition frequency were matched to the resonance frequency of that mode, we can actually anticipate an enhancement in the IC process so that one could realize a large number of electrons from a large sample of excited nuclei placed at that location. A large sample should be possible since for the lowest mode numbers there will be little variation in the cavity wave functions over the location of the nuclei so a larger packing density could be achieved.

As noted above, the IC process is generally dominated by the virtual photon exchange mechanism. A virtual transverse photon is emitted and immediately absorbed. However, in the instance where we completely suppress the IC process, excursions of the electrons into the K-shell and the Coulomb processes become more critical to the IC process. The transition matrix element with the Coulomb forces between the nuclei and the electrons present has the form

$$\langle \Psi_f | \hat{H}_{int} | \Psi_i \rangle = \langle \Psi_f | \hat{H}^{(2)}_{int} | \Psi_i \rangle + \langle \psi_\beta \phi_f \left| \frac{\rho_N(\vec{x}_N)\rho_e(\vec{x}_e)}{|\vec{x}_N - \vec{x}_e|} \right| \phi_i \psi_\alpha \rangle. \quad (51)$$

As shown in Ref. 22 for the free-space case, the transverse photon terms cancel the longitudinal photon contributions except for the spherically symmetric modes, the largest contribution coming from the $\mathcal{L} = 0$ mode. It is also shown there that these longitudinal photon contributions are generally quite small in comparison to the transverse photon values. This is also true for the cavity case. The eigenfunctions for the potential in a cavity which are zero on all the walls have the form

$$\Phi_{nlm}(\vec{x}) = \left(\frac{8}{\pi^2 L}\right)^{1/2} \sin\left(\frac{n\pi}{L}x\right) \sin\left(\frac{l\pi}{L}y\right) \sin\left(\frac{m\pi}{L}z\right). \quad (52)$$

Thus the Green's function for the Poisson equation in this cavity yields

$$\begin{aligned}
&\langle \psi_\beta \phi_f \left| \frac{\rho_N(\vec{x}_N)\rho_e(\vec{x}_e)}{|\vec{x}_N - \vec{x}_e|} \right| \phi_i \psi_\alpha \rangle \\
&= \sum_{n,l,m=1}^{\infty} \frac{1}{n^2 + l^2 + m^2} \int d^3\vec{x} \rho^N_{\alpha\beta}(\vec{x}) \Phi_{nlm}(\vec{x}) \int d^3\vec{x}' \rho^e_{if}(\vec{x}') \Phi_{nlm}(\vec{x}') \\
&\sim \sum_{n,l,m=1}^{\infty} \frac{1}{n^2 + l^2 + m^2} \Phi_{nlm}(\vec{x}_N) \left[\int d^3\vec{x} \rho^N_{\alpha\beta}(\vec{x}) \right] \int d^3\vec{x}' \rho^e_{if}(\vec{x}') \Phi_{nlm}(\vec{x}').
\end{aligned} \quad (53)$$

Since $\rho^N_{\alpha\beta}(\vec{x})$ is expandable into spherical harmonics, the integration in the first brackets is zero except for spherically symmetric modes. The largest value yielded is for the $\mathcal{L} = 0$ mode. Nonetheless, we see that if the transverse photons are completely suppressed by the location of the nucleus, then additionally the longitudinal photon or Coulomb

contribution will be completely suppressed. The Coulomb terms can also be made negligible by the choice of the nuclei. For instance, the $\mathcal{L} = 0$ transition is very rare for the choice of a long-lived spin isomeric state. We will make such a choice for all of the applications considered below.

3.3 Proof-of-Concept Experiment

To test the efficacy of suppressing the IC process, we consider a cavity that has a side length $L = 10.0\ nm = 100\ \text{Å}$. This length corresponds to an energy of 124 eV. The $\{1,\ 0,\ 0\}$-mode will correspond to this wavelength. The $\{10,\ 0,\ 0\}$-mode would correspond to an energy of 1.24 keV. The mode separation in this cavity $d(\hbar\omega_{nlm})/dn = \hbar c/(nL)$ for these modes is, respectively, $\sim 100\ eV$ and $\sim 10\ eV$. The Q of this cavity is related to the width of the transition by $\Gamma \sim (\hbar\omega_{nlm})/Q$. Thus in either of these two-cases one would need $Q \sim 10$–100 to have a line width much smaller than the transition frequency. We believe that cavities of this size and this Q for the indicated transition frequencies are possible with current micro-fabrication processes [25]. In particular, it appears [26] that a cavity with a suitable Q can be constructed for transitions near the 1.0 keV range with crystals or for energies below 10.0 eV with high-energy multilayer mirror components, but not in the range between 10–100 eV. These constraints in turn require the selection of nuclear isomers with transitions near 1.0 keV and below 10.0 eV. The cavity would then be constructed in such a manner that it is grown with a large number of nuclei of those isomers embedded at selected locations. This would provide the conditions necessary for the complete suppression of the IC process. Measurement of the IC transition rates could then be made. Sensitivity to the location of the nuclei could be tested by constructing these cavities with the nuclei embedded in other specified locations.

Such an experiment would require some additional analyses. Rectangular cavities would be much easier to fabricate. This would require redoing the above IC analyses using the cavity lengths L_x, L_y, L_z. The experimental choices of the modes to be used, their separations, and the relationships to the actual Q of the lossy cavity should be modeled. This can be achieved with a variety of available computational electromagnetic simulators. Issues of adequate mode separation may be critical to minimize the available channels for the IC process to occur.

4. POTENTIAL APPLICATIONS

There are several potential practical uses for localized excited nuclei which have their IC decay process suppressed. These include long-term containment of excited nuclear material, high energy nuclear batteries, and neutron detectors.

4.1 Containment of Excited Nuclei

One very interesting application of the suppression of the IC process would be the ability to store excited nuclei for long periods of time. In fact, one could anticipate a nano- or micron-sized closed cavity with walls fabricated with multilayers to form a photonic band-gap structure tuned to the virtual photon emission frequency. Then one would have to embed a large number of nuclei in this closed cavity and excite them by transporting an energetic neutron beam through the walls. If the cavity Q is immense, the nuclei will remain in their resulting excited states almost indefinitely if their IC and SpE rates are suppressed.

4.2 Nuclear Battery

Since we can now control the IC and SpE rates of the nuclei, let us consider a partially open, high Q cavity with a large number of nuclei embedded within it, say a cubical cavity with two small circular apertures on one pair of juxtaposed sides. We drive the nuclei into their excited states with a neutron beam entering the cavity through those apertures. If the nuclei are positioned on a peak of the divergence of the cavity modal coefficients, we can enhance the emission rate of electrons from the nuclei. If we were to superimpose a static magnetic field over the cavity orthogonal to two suspended metallic collection plates within the cavity, the emitted electrons would be directed by the magnetic field towards these collection plates and could then be captured by them. These excess electrons can then be used to drive currents in an external circuit connected to the collector plates. This process is essentially a neutron to electron convertor. The nuclei-cavity system thus acts as a source of a large number of electrons, hence, is a large current battery. This nuclear battery configuration is shown in Figure 2.

Another variation would be to emit the electrons more slowly with a controlled rate so that a low current battery could be obtained. This could be accomplished by modifying appropriately the size of

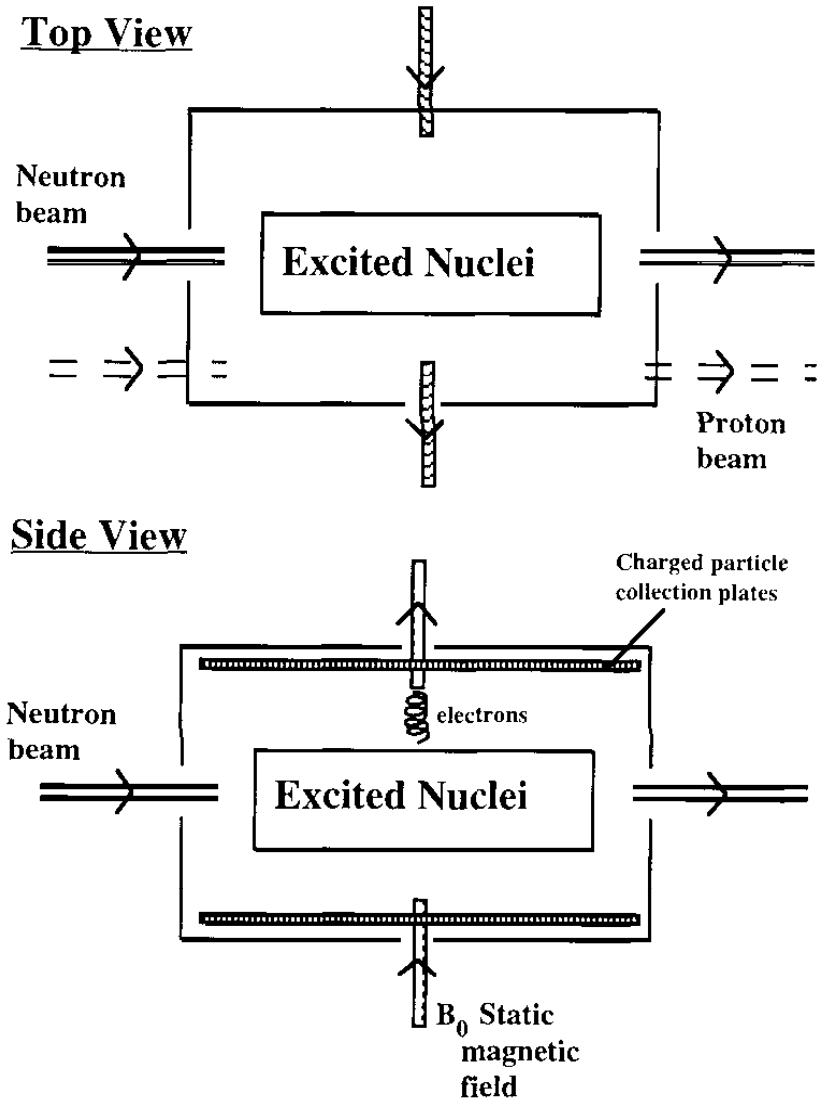

Figure 2. Nuclear battery configuration.

the cavity, hence, its modal coefficients. This size modification could be achieved by driving the cavity with an energetic proton beam introduced in an offset position (through another juxtaposed pair of apertures) which would effectively short-out the cavity at the position of the proton beam. The rate of emission of the electrons could then be modulated directly in such a configuration with a modulated proton beam.

4.3 Neutron Detector

The nuclear battery configuration could also act as a neutron detector. Consider a partially open cavity containing nuclei in their ground state that are located at the peaks of the divergences of the modal coefficients. If these nuclei are exposed to a beam of neutrons that excite them, they will quickly emit electrons via the IC process. The collector plates would then collect these electrons and a current would be measured that was directly proportional to the number of neutrons in the beam. This system would act like a photomultiplier tube which converts photons into electrons.

5. CONCLUSIONS

We have shown in this paper that one can control the major mechanisms leading to the decay of excited nuclei by controlling the electromagnetic environment into which they must radiate either virtual or real photons. It was demonstrated that the value of the IC matrix elements for a nucleus in a cavity will be highly dependent on the position of the nuclei in the cavity. By simply locating the nuclei at a null or at a peak of the cavity modal coefficients, one can inhibit or enhance the IC electron emission rate. These results obviously imply that the presence of the cavity walls can significantly alter the IC process. This occurs even though the exchange process involves a virtual photon emission and reabsorption. A proof-of-concept experiment was suggested to test these suppression and enhancement results.

Several potential applications for nuclei with their IC processes suppressed or enhanced were suggested. These applications require the construction of extremely small cavities with walls that have a high Q at large photon energies. Such cavities appear to be within reach of current fabrication methods dealing with multilayers or crystals to form photonic band-gap structures. However, we fully appreciate the practical difficulties of achieving these requisite high Q's at the photon energies associated with nuclear transitions. We are currently analyzing such multilayer cavities in the anticipation of providing some ideas as to what material parameters will be required and how they may be designed effectively for these applications. While the theoretical possibility of the suppression of the nuclear IC process has been demonstrated here, its ultimate practical realization and the ability to achieve the proposed applications rests on the success of designing and

fabricating these cavities. Nonetheless, we hope the theoretical possibility of suppressing the nuclear IC process will stimulate experimental interest.

As we noted in the introduction, another virtual photon (radiationless) process that may be suppressed in a cavity environment is the one associated with Auger transitions in an atom. The suppression of this atom-electron process may also be of interest for the development of a near-term proof-of-concept experiment. Since they deal with lower energy photons than those associated with the nucleus-electron IC process, one could deal with these Auger transitions to reduce substantially the demands on a realizable cavity from those required for an IC suppression experiment. This possibility is also currently under investigation.

APPENDIX A: QUANTUM CALCULATION OF Q

Previously we defined the broadening of the cavity modes due to the coupling of the EM field with the walls:

$$\omega_{nlm} = \omega^R_{nlm} - i\Gamma_{nlm} \tag{A.1}$$

where

$$\Gamma_{nlm} = \frac{\sum_\epsilon \int\int \mathrm{Re}(Z_{wall})|\vec{H}^\epsilon_{nlm}|^2\, dS}{\mu_0 \sum_\epsilon \int\int\int |\vec{H}^\epsilon_{nlm}|^2\, d^3\vec{x}} \tag{A.2}$$

This result can be generated by inserting into the expression $\mu_0\vec{H} = \mathrm{rot}\vec{A}$ the definition of the cavity vector potential (2). With a slight manipulation of the coefficients one obtains

$$\vec{A}(\vec{x},t) = \sum_{\substack{nlm \\ \epsilon}} \vec{K}^\epsilon_{nlm}(\vec{x}) e^{i\omega_{nlm}t} A^{(\epsilon)}_{nlm} + c.c. \tag{A.3}$$

where

$$\vec{K}^\epsilon_{nlm}(\vec{x}) = \mu_{nlm}\vec{G}^\epsilon_{nlm}(\vec{x}) \tag{A.4a}$$

$$\mu_{nlm} = \left(\frac{\hbar}{2\epsilon_0 C_\epsilon \omega_{nlm}}\right)^{1/2} \tag{A.4b}$$

The definition of $\vec{G}^\epsilon_{nlm}(\vec{x},t)$ is given in terms of the F_{nlm}. The resulting expansion for $\vec{K}^\epsilon_{nlm}$ then takes the form

$$\vec{K}^\epsilon_{nlm}(\vec{x}) = \sum_i \alpha^{\epsilon,i}_{nlm} F_{nlm}(\vec{x}) e_i \tag{A.5}$$

the e_i are the unit vectors in rectangular coordinates and the coefficients:

$$\alpha^{1,1}_{nlm} = -\mu^{\epsilon}_{nlm}\delta_{\epsilon 1} \tag{A.6a}$$

$$\alpha^{1,2}_{nlm} = N_{nlm}\mu^{\epsilon}_{nlm}\left[\frac{l}{n}\delta_{\epsilon 1} + \frac{m}{n}\delta_{\epsilon 2}\right] \tag{A.6b}$$

$$\alpha^{1,3}_{nlm} = N_{nlm}\mu^{\epsilon}_{nlm}\left[\frac{m}{n}\delta_{\epsilon 1} - \frac{l}{n}\delta_{\epsilon 2}\right] \tag{A.6c}$$

$$\alpha^{2,1}_{nlm} = -n\mu^{\epsilon}_{nlm} \tag{A.6d}$$

$$\alpha^{2,2}_{nlm} = lN_{nlm}\mu^{\epsilon}_{nlm} \tag{A.6e}$$

$$\alpha^{2,3}_{nlm} = mN_{nlm}\mu^{\epsilon}_{nlm} \tag{A.6f}$$

The expression of the components of the magnetic field $\vec{H}$ can be written now as

$$\mu_0 H^{\epsilon,j}_{nlm} = \alpha^{\epsilon,j}_{nlm}\nabla_k F^j_{nlm} - \alpha^{\epsilon,k}_{nlm}\nabla_j F^k_{nlm} \tag{A.7}$$

Using the expressions for the F^j_{nlm}, we find

$$\mu_0 H^{\epsilon,1}_{nlm} = \left(\frac{2}{L}\right)^{3/2}\frac{\pi}{L}[l\alpha^{\epsilon,3}_{nlm} - m\alpha^{\epsilon,2}_{nlm}]\sin\left(\frac{n\pi}{L}x\right)\cos\left(\frac{l\pi}{L}y\right)\cos\left(\frac{m\pi}{L}z\right) \tag{A.8a}$$

$$\mu_0 H^{\epsilon,2}_{nlm} = \left(\frac{2}{L}\right)^{3/2}\frac{\pi}{L}[m\alpha^{\epsilon,1}_{nlm} - n\alpha^{\epsilon,3}_{nlm}]\cos\left(\frac{n\pi}{L}x\right)\sin\left(\frac{l\pi}{L}y\right)\cos\left(\frac{m\pi}{L}z\right) \tag{A.8b}$$

$$\mu_0 H^{\epsilon,3}_{nlm} = \left(\frac{2}{L}\right)^{3/2}\frac{\pi}{L}[n\alpha^{\epsilon,2}_{nlm} - l\alpha^{\epsilon,1}_{nlm}]\cos\left(\frac{n\pi}{L}x\right)\cos\left(\frac{l\pi}{L}y\right)\sin\left(\frac{m\pi}{L}z\right) \tag{A.8c}$$

The power loss in the walls is obtained by a surface integral over only the walls of the cavity. On the other hand, the energy is a volume integral over the entire cavity. These quantities can now be calculated and yield

$$\begin{aligned}\sum_{\epsilon}\int\int |\vec{H}^{\epsilon}_{nlm}|^2 dS &= 2\sum_i \int_0^L\int_0^L dS_i \sum_{i\neq j}|\vec{H}^{\epsilon,j}_{nlm}|^2_{x_i=0} \\ &= \frac{8}{L}\frac{\hbar\omega^R_{nlm}}{\mu_0}\end{aligned} \tag{A.9a}$$

$$\mu_0 \sum_{\epsilon} \int\int\int |\vec{H}^{\epsilon}_{nlm}|^2 d^3\vec{x} = \hbar\omega^R_{nlm} \tag{A.9b}$$

Therefore the transition loss-width is:

$$\Gamma_{nlm} = \frac{8\mathrm{Re}(Z_{wall})}{\mu_0 L} = \frac{8\mathrm{Re}(Z_{wall})}{\sqrt{\epsilon_0\mu_0}L}\sqrt{\frac{\epsilon_0}{\mu_0}} = 8\left(\frac{c}{L}\right)\frac{\mathrm{Re}(Z_{wall})}{Z_0} \tag{A.10}$$

where $Z_0 = (\mu_0/\epsilon_0)^{1/2}$ is the characteristic wave impedance of free space. Notice that the dimension of Γ_{nlm} is the same as inverse time. This means the quantum mechanical Q of the cavity is

$$Q = \frac{\omega^R_{nlm}}{\Gamma_{nlm}} = \frac{3\pi}{2}\frac{Z_0}{\mathrm{Re}(Z_{wall})}\frac{\text{volume of cavity}}{\text{interior surface area of cavity}}\frac{1}{\lambda^R_{nlm}}. \tag{A.11}$$

This shows that the cavity Q increases with the mode number or correspondingly with the cavity size. For cavity walls made from very good metallic, conducting metals

$$\mathrm{Re}(Z_{wall}) = \sqrt{\frac{\omega^R_{nlm}\mu_0}{2\sigma}} \tag{A.12}$$

so that the line-width

$$\Gamma_{nlm} = \frac{\sqrt{32}}{\mu_0 L}\sqrt{\frac{\omega^R_{nlm}\mu_0}{\sigma}} \tag{A.13a}$$

and the cavity's

$$Q = \frac{L}{\sqrt{32}c}\sqrt{\frac{\sigma}{\epsilon_0}}\sqrt{\omega^R_{nlm}} \tag{A.13b}$$

These results indicate that the quantum mechanical Q increases with increasing conductivity and mode number (i.e., from (A.11) we know that Q increases as the ratio of the cavity volume to its surface area) as it does classically (see Appendix B).

APPENDIX B: CLASSICAL CALCULATION OF Q

A classical cavity with lossy walls acts like a lossy resonator circuit: i.e., a circuit consisting of a capacitance C, and inductance L, and a

conductance $G = 1/R_{wall}$ in parallel, R_{wall} being the wall resistance, driven by a voltage source of strength V_0 at the frequency ω. The total impedance seen by this source is thus

$$Z_{total} = \left[G - i\left(\omega C - \frac{1}{\omega L}\right)\right]^{-1} \tag{B.1}$$

At resonance the electric and magnetic energies are equal so that $W_{stored} = 2W_e = 2W_m = CV_0^2 = LI_0^2$. The power loss in the walls is simply $P_{loss} = GV_0^2$. Therefore the Q of the cavity is

$$Q = \frac{\omega_0 W_{stored}}{P_{loss}} = \omega_0 \frac{C}{G} \tag{B.2}$$

where the resonant frequency $\omega_0^{-1} = \sqrt{LC}$. The total wall impedance can then be rewritten as

$$Z_{wall} = iR_{wall} \frac{\omega(\omega_0/Q)}{\omega^2 - \omega_0^2 + i\omega(\omega_0/Q)} \tag{B.3}$$

If we identify the line-width of the resonance to be its full width at half-maximum and denote it as Γ_{FWHM}, we find that (B.3) gives

$$\Gamma_{FWHM} = 2\frac{\omega_0}{Q}. \tag{B.4}$$

If the source frequency ω is tuned near the resonance ω_0, the impedance can now be rewritten as

$$Z_{wall} \approx \frac{i}{2} R_{wall} \frac{(\Gamma_{FWHM}/2)}{\omega - \omega_0(1 - i\,\Gamma_{FWHM}/2\omega_0)}. \tag{B.5}$$

If we set $\Gamma_0 = \frac{\Gamma_{FWHM}}{2}$, this means the circuit now can be viewed as having a resonance frequency

$$\omega \sim \omega_0(1 - i\,\Gamma_{FWHM}/2\omega_0) = \omega_0(1 - i/Q) = \omega_0 - i\,\Gamma_0 \tag{B.6}$$

as was determined in the quantum mechanical calculation. Note that these results can be obtained directly from the equivalent classical electromagnetic field expressions. In particular we note that the line width of the nlm-mode is

$$\Gamma_{nlm} = \frac{\iint \mathrm{Re}(Z_{wall})|\vec{H}_{nlm}|^2}{\mu_0 \iiint |\vec{H}_{nlm}|^2 d^3\vec{x}}.$$

Recall from Appendix A that this is the same, modulo the sum over the equally probable polarization states, as the quantum mechanical expression.

APPENDIX C: Q OF A CAVITY HAVING LORENTZ MEDIUM WALLS

For cavity walls consisting of a Lorentz medium, the associated polarization vector satisfies the damped harmonic oscillator equation:

$$\frac{d^2}{dt^2}\vec{P} + \Gamma_L \frac{d}{dt}\vec{P} + \omega_0^2 \vec{P} = \epsilon_0 \omega_p^2 \vec{E} \tag{C.1}$$

where the plasma frequency $\omega_p = N_{atom} e^2/m\epsilon_0$ and the polarization $\vec{P} = -N_{atom} e\vec{x}$. The corresponding polarization current is $\vec{J} = \partial_t \vec{P}$.

For a time harmonic driving field with angular frequency ω, this means $\vec{J}_\omega = -i\omega \vec{P}_\omega$ and

$$\vec{P}_\omega = \frac{\epsilon_0 \omega_p^2}{\omega_0^2 - \omega^2 - i\omega\ \Gamma_L} \vec{E}_\omega \equiv \epsilon_0(\chi_r + i\chi_{im})\vec{E}_\omega \tag{C.2}$$

where the complex amplitude quantities are labeled explicitly by the angular frequency.

If we now identify the conductivity of the walls as

$$\sigma_{wall} = \vec{J}_\omega / \vec{E}_\omega = -i\omega \vec{P}_\omega / \vec{E}_\omega = \epsilon_0 \omega(\chi_{im} - i\chi_r) \tag{C.3}$$

the average power loss density in the walls is

$$\begin{aligned} P_{loss} =& \frac{1}{2}\mathrm{Re}(\vec{J}_\omega \cdot \vec{E}_\omega^*) = \frac{1}{2}\mathrm{Re}(\sigma_{wall}|\vec{E}_\omega|^2) \\ =& \frac{1}{2}\mathrm{Re}(\sigma_{wall})|\vec{E}_\omega|^2 = \left[\frac{1}{2}\epsilon_0 |\vec{E}_\omega|^2\right] \omega\chi_{im} \end{aligned} \tag{C.4}$$

The average energy stored in the cavity is

$$W_{stored} = \frac{1}{2}\iiint d^3\vec{x}\, \epsilon_0 |\vec{E}_\omega|^2 \tag{C.5}$$

Again, at a resonance the stored electric and magnetic energy densities are equal; i.e., $(1/2)\epsilon_0|\vec{E}_\omega|^2 = (1/2)\mu_0|\vec{H}_\omega|^2$ so that the line width associated with the cavity losses is simply.

$$\Gamma_{wall} = \frac{\iint_{cavity\ walls} dS\ P_{loss}}{W_{stored}} = \frac{\iint dS(\omega\chi_{im})|\vec{H}_\omega|^2}{\iiint d^3\vec{x}|\vec{H}_\omega|^2} \tag{C.6}$$

This quantity is completely determined in terms of the imaginary part of the susceptibility of the walls

$$\chi_{im} = \frac{\omega\,\Gamma_L}{(\omega_0^2-\omega^2)^2+(\omega\,\Gamma_L)^2}\omega_p^2, \tag{C.7}$$

where Γ_L is the line-width associated with the transition in the wall medium. Near a resonance ω_0 of the wall medium one then has

$$\Gamma_{wall} \sim \omega_0\chi_{im} \approx \frac{\omega_p^2}{\Gamma_L} \tag{C.8}$$

This means the $Q = \omega_{nlm}^R/\Gamma_{wall}$ of the cavity mode associated with the angular frequency ω_{nlm}^R will be proportional to

$$Q \sim \omega_{nlm}^R\Gamma_L/\omega_p^2. \tag{C.9}$$

Thus if the line width of the wall transitions is large (small) in comparison to the resonant frequency of the cavity, the cavity's Q will be large (small). In general, we expect that the linewidths, hence, the cavity's Q will be small if the walls appear as dielectrics to the cavity fields, i.e., if the resonant frequency is very high and the electrons in the walls can not respond fast enough to the fields.

APPENDIX D: NUCLEAR CURRENT MATRIX ELEMENT

We need to calculate explicitly the matrix element (48a) for the cavity-enclosed nucleus, which we repeat here for convenience:

$$X_{\beta\alpha}(nlm;\,\epsilon) = \left(\frac{\hbar}{2\epsilon_0\omega_{nlm}}\right)^{1/2}\int d^3\vec{x}'\langle\psi_\beta|\vec{j}_N^{\perp}(\vec{x}')\cdot\vec{G}_{nlm}^{(\epsilon)}(\vec{x}')|\psi_\alpha\rangle. \tag{D.1}$$

The nuclear current operator $\vec{j}_N^{\perp}$ has the form

$$\vec{j}_N^{\perp}(\vec{x}) = -i\hbar\left(\frac{q}{M}\right)_N\sum_i\delta(\vec{x}'-\vec{x}_i)\nabla_{\vec{x}_i}, \tag{D.2}$$

where the $\vec{x}_i$ are the locations of the nucleons in the nucleus. The matrix element in (D.1) then becomes

$$\langle\psi_\beta|\vec{j}^{\perp}_N(\vec{x}')|\psi_\alpha\rangle = - i\hbar\left(\frac{q}{M}\right)_N \sum_i \int d^3\vec{x}_1 \ldots d^3\vec{x}_i \ldots d^3\vec{x}_n \; \psi^*_\beta(\vec{x}_1,\ldots,\vec{x}_i,\ldots,\vec{x}_n) \times \delta(\vec{x}' - \vec{x}_i)\nabla_{\vec{x}_i}\psi_\alpha(\vec{x}_1,\ldots,\vec{x}_i,\ldots,\vec{x}_n) d^3\vec{x}_1 \ldots d^3\vec{x}_i \ldots d^3\vec{x}_n, \tag{D.3}$$

where $\vec{x}_1,\ldots,\vec{x}_i,\ldots,\vec{x}_n$ are the positions of the n nucleons in the nuclei. Therefore the IC matrix element

$$X_{\beta\alpha}(nlm;\ \epsilon) = - i\hbar\left(\frac{q}{M}\right)_N \left(\frac{\hbar}{2\epsilon_0\omega_{nlm}}\right)^{1/2} \sum_i \int d^3\vec{x}' d^3\vec{x}_1 \ldots d^3\vec{x}_i \ldots d^3\vec{x}_n \; \vec{G}^{(\epsilon)}_{nlm}(\vec{x}_i) \times [\psi^*_\beta(\vec{x}_1,\ldots,\vec{x}_i,\ldots,\vec{x}_n)\delta(\vec{x}' - \vec{x}_i)\nabla_{\vec{x}_i}\psi_\alpha(\vec{x}_1,\ldots,\vec{x}_i,\ldots,\vec{x}_n)]. \tag{D.4}$$

Consequently, because the vector potential in the cavity varies slowly over the dimensions of the nucleus located at $\vec{x}_N$, we can extract the field coefficients $\vec{G}^{(\epsilon)}_{nlm}$ from the integral to obtain

$$X_{\beta\alpha}(nlm;\ \epsilon) \approx -i\hbar\left(\frac{q}{M}\right)_N \left(\frac{\hbar}{2\epsilon_0\omega_{nlm}}\right)^{1/2} \vec{G}^{(\epsilon)}_{nlm}(\vec{x}_N) \times \sum_i \int d^3\vec{x}_1 \ldots d^3\vec{x}_i \ldots d^3\vec{x}_n \left[\psi^*_\beta(\vec{x}_1,\ldots,\vec{x}_i,\ldots,\vec{x}_n)\delta(\vec{x}' - \vec{x}_i) \times\nabla_{\vec{x}_i}\psi_\alpha(\vec{x}_1,\ldots,\vec{x}_i,\ \ldots,\vec{x}_n)\right] \tag{D.5}$$

where the nucleon locations $\vec{x}_i = \vec{x}_N + \vec{\xi}_i$, $|\vec{\xi}_i| \ll |\vec{x}_N|$. We introduce the nucleon transition current

$$\vec{J}_{\beta\alpha} = -i\hbar\left(\frac{q}{M}\right)_N \sum_i \int d^3\vec{x}' d^3\vec{x}_1 \ldots d^3\vec{x}_i \ldots d^3\vec{x}_n \left[\psi^*_\beta(\vec{x}_1,\ldots,\vec{x}_i,\ldots,\vec{x}_n) \times \delta(\vec{x}' - \vec{x}_i)\nabla_{\vec{x}_i}\psi_\alpha(\vec{x}_1,\ldots,\vec{x}_i,\ \ldots,\vec{x}_n)\right], \tag{D.6}$$

to write

$$X_{\beta\alpha}(nlm;\ \epsilon) \approx \left(\frac{\hbar}{2\epsilon_0\omega_{nlm}}\right)^{1/2} \vec{G}^{(\epsilon)}_{nlm}(\vec{x}_N)\cdot\vec{J}_{\beta\alpha}. \tag{D.7}$$

As a result, we can control the values of the IC matrix elements through the location of the nuclei in the cavity. In particular, for instance, if the nucleus is located at the center of the cavity so that $\vec{x}_N = (L/2,\ L/2,\ L/2)$, then we know from Eqs. (1a)–(5f) that

$$\vec{G}^{(\epsilon)}_{nlm}(\vec{x}_N) \equiv 0; \tag{D.8}$$

and thus, the IC matrix element will be zero. It is clear that the value of the resulting IC matrix elements will be highly position dependent. These results obviously imply that the presence of the cavity walls can significantly alter the rates of the IC process.

ACKNOWLEDGMENT

The authors would like to thank Marc Launois, a former director of the C.E.A./C.E.S.T.A. facility in Le Barp, France for making this binational collaboration possible.

REFERENCES

1. Purcell, E. M., *Phys. Rev.*, Vol. 69, 681, 1946.
2. Milonni, P. W. and P. L. Knight, *Opt. Comm.*, Vol. 9, 119, 1973.
3. Kleppner, D., *Phys. Rev. Lett.*, Vol. 47, 233, 1981.
4. Cook, R. J. and P. W. Milonni, *Phys. Rev. A*, Vol. 35, 5081, 1987.
5. Parker, J. and C. R. Stroud, Jr., *Phys. Rev. A*, Vol. 35, 4226, 1987.
6. Brorson, S. D., H. Yokotama, and E. P. Ippen, *IEEE J. Quan. Electron.*, Vol. 26, 1492, 1990.
7. Dowling, J. P., M. O. Scully, and F. DeMartini, *Opt. Comm.*, Vol. 118, 415, 1991.
8. Seeley, F. B., J. E. Alexander, R. W. Connaster, and J. S. Conway, *Am. J. Phys.*, Vol. 61, 545, 1993.
9. Rempe, G., *Contemp. Phys.*, Vol. 34, 119, 1993.
10. Dowling, J. P., *Found. Phys.*, Vol. 12, 895, 1993.
11. Björk, G., *IEEE J. Quan. Electron.*, Vol. 30, 2314, 1994.
12. Miloni, P. W., *The Quantum Vacuum*, Boston: Academic Press, 1994.
13. Keitel, C. H., P. L. Knight, L. M. Narducci, and M. O. Scully, *Opt. Comm.*, Vol. 118, 143, 1995.
14. Cheon, I.-T., *J. Phys. Soc.*, Japan, Vol. 60, 833, 1991.
15. Cheon, I.-T., *J. Phys. Soc.*, Japan, Vol. 61, 2257, 1992.

16. Cheon, I.-T., *J. Phys. Soc.*, Japan, Vol. 62, 4240, 1993.
17. Fischbach, E., and N. Nakagawa, *Phys. Lett.*, Vol. 149B, 504, 1984.
18. Kol'tsov, V. V., and A. A. Rimskii-Korsakov, *Izvestiya Akademii Nauk SSSR, Seriya Fizichaskaya*, Vol. 53, 2085, 1989.
19. Voryhalov, O. V., E. A. Zaitsev, V. V. Kol'tsov, and A. A. Rimskii-Korsakov, *Bull. Russ. Acad. Sci.*, Vol. 56, 81, 1992.
20. Artna-Cohen, A., *J. Quant. Spectrosc. Radiat. Transfer*, Vol. 40, 663, 1988.
21. Cohen-Tannoudji, C., J. Dupont-Doc, and G. Grynberg, *Processus d'interaction entre photons et atomes*, Paris, France: Inter Editions, 24–37, 1988.
22. Pauli, H. C., K. Adler, and R. M. Steffen, *The Electromagnetic Interaction in Nuclear Spectroscopy*, Ch. 10, Ed. W. D. Hamilton, Amsterdam: North-Holland Publ. Co., 341 -440, 1975.
23. Ziolkowski, R. W. and W. A. Johnson, *J. Math. Phys.*, Vol. 26, 1293, 1987.
24. Ziolkowski, R. W. and D. P. Marsland, L. F. Libelo, and G. Pisane, *IEEE Trans. Antennas and Propagat.*, Vol. AP-36, 985, 1988.
25. Dhex, P., *Ann. Phys. Fr.*, Vol. 15, 493, 1990.
26. Falco, Charles, private communications, Department of Physics, University of Arizona, November 1996.